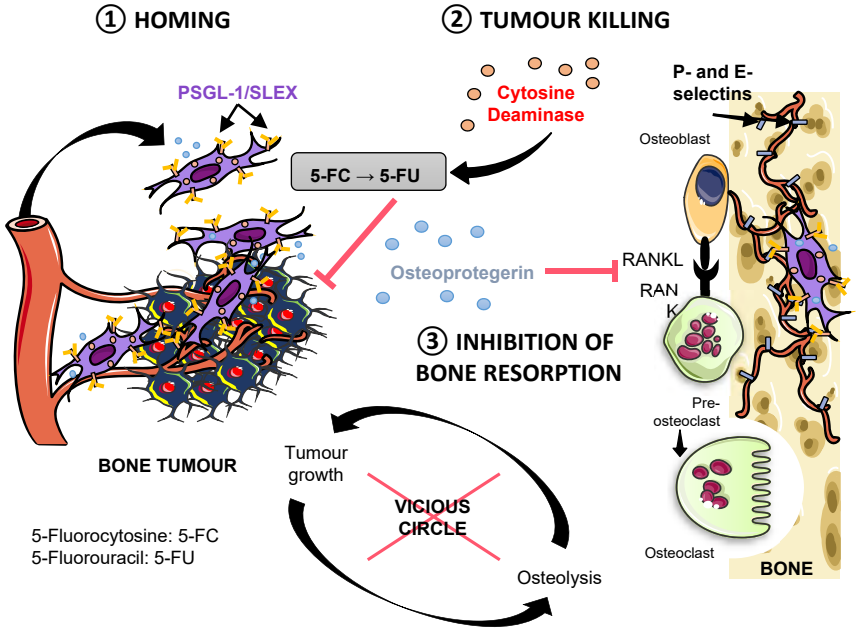

Figure 1: Combinatorial targeting of cancer bone metastasis using mRNA engineered mesenchymal stem cells. Proposed strategy for bone metastasis treatment by targeted delivery of multiple factors using mRNA-engineered mesenchymal stem cell (MSC) equipped with functions for a) specific and efficient bone metastases homing through P-selectin glycoprotein ligand-1 (PSGL-1) and Sialyl-Lewis X (SLEX), b) local cancer killing through cytosine deaminase (CD)/pro-drug 5-Fluorocytosine, and c) osteolysis inhibition within the tumour niche through a modified version of RANKL decoy receptor, osteoprotegerin (OPG).

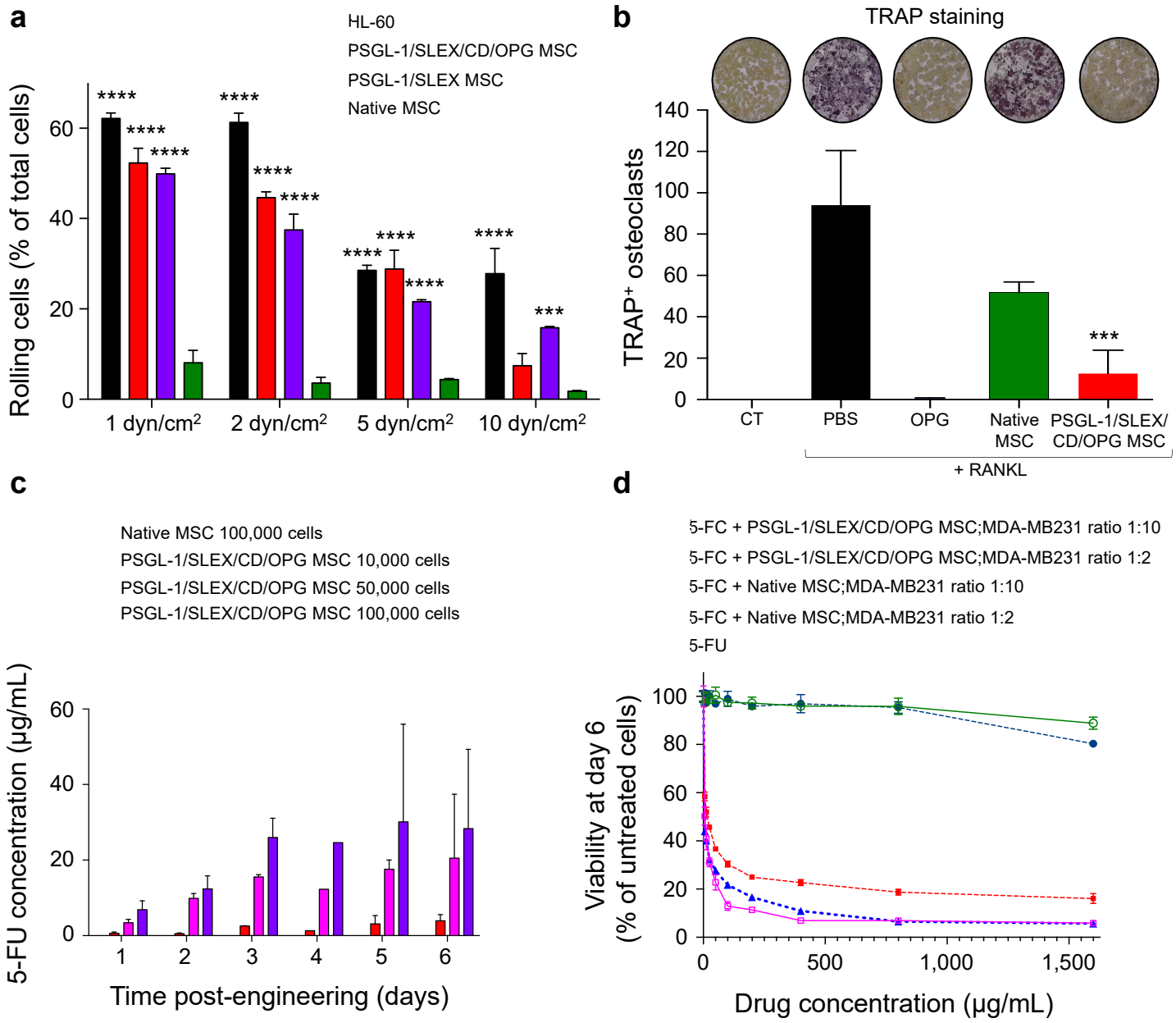

Figure 2: MSC engineering using mRNA and *in vitro* functional validation. (a) PSGL-1/SLEX/CD/OPG MSC display functional rolling on an endothelial layer under physiological shear flow. Native MSC, PSGL-1/SLEX MSC and PSGL-1/SLEX/CD/OPG MSC were flowed on a layer of endothelial cells at different physiological flow-rates 24 h post-MSC engineering. HL-60 leukocytic cells were used as a positive control for rolling. Plot: mean + SD, statistical analysis: Two-way ANOVA test with Dunnett's multiple comparison test to compare each column to Native MSC, *** $p \leq 0.001$, **** $p \leq 0.0001$. (b) PSGL-1/SLEX/CD/OPG MSC inhibit osteoclastic differentiation *in vitro*. Murine osteoclast precursors (RAW264.7 cells) were plated for 6 days in media with the addition of nothing (CT), 100 ng/mL recombinant murine RANKL to induce osteoclastogenesis, and day 2 supernatant of MSC (Native and PSGL-1/SLEX/CD/OPG). 100ng/mL of recombinant human OPG was used as a positive control for osteoclastogenesis inhibition. Pictures show the TRAP stained culture at day 6 for each condition. Plot: mean + SD, statistical analysis: Kruskal-Wallis with Dunn's multiple comparison test, *** $p \leq 0.001$ compared to PBS+RANKL condition. (c) PSGL-1/SLEX/CD/OPG MSC convert 5-FC into 5-FU *in vitro* in a cell concentration-dependent manner. 24 h post-engineering, MSC were plated at different concentrations in presence of 400 µg/mL 5-FC. LC-MS/MS was done on conditioned media collected at different days to measure the 5-FU converted from 5-FC. Plot shows mean + SD. (d) PSGL-1/SLEX/CD/OPG MSC kill MDA-MB231 cancer cells *in vitro*. Native MSC and PSGL-1/SLEX/CD/OPG MSC were plated at different ratios (1:2 and 1:10) on top of cancer cells in the presence of increasing doses of 5-FC, and the viability of the co-culture was determined at day 6. 5-FU was used as a positive control. Graph shows mean ± SD.

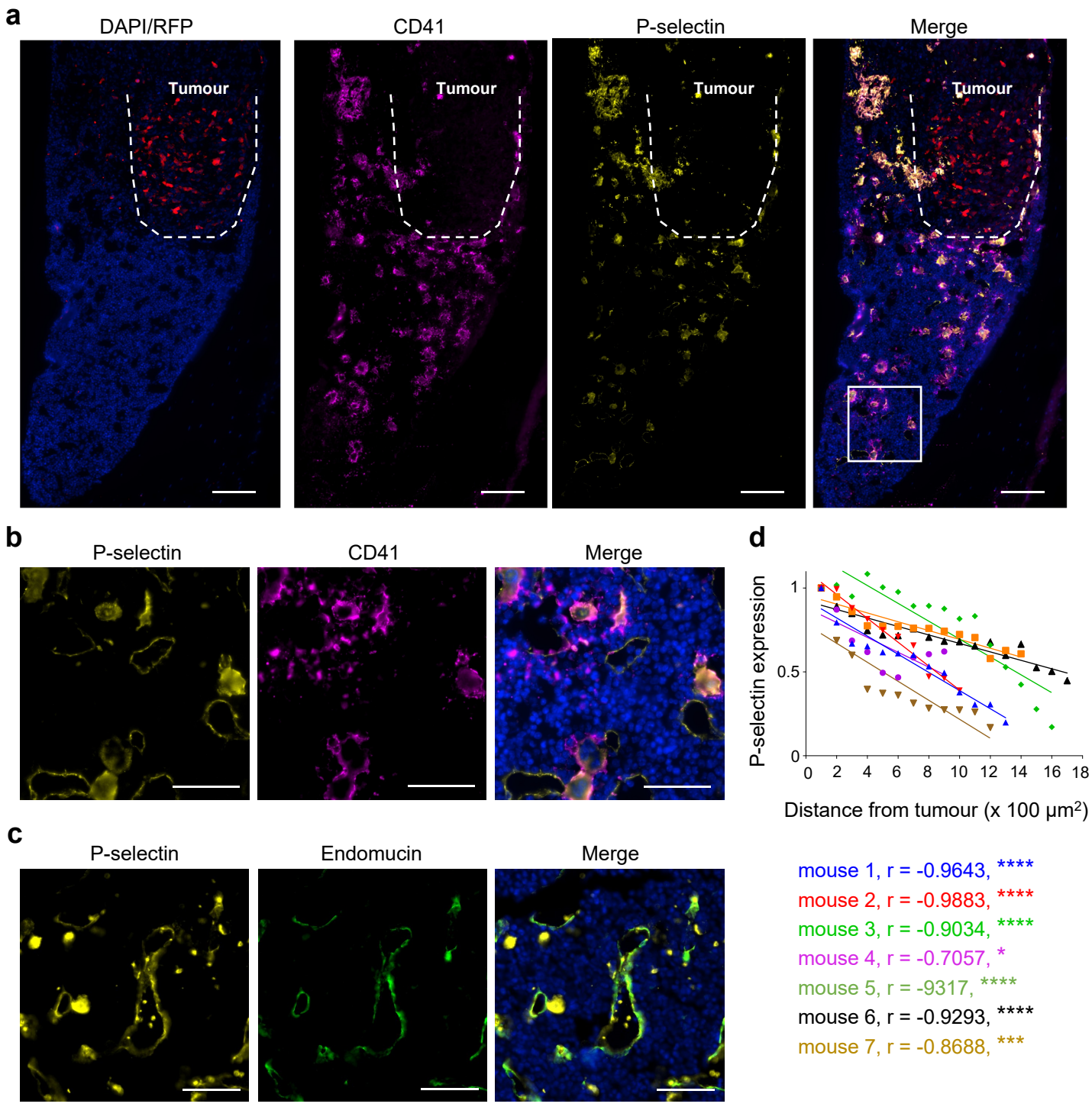

Figure 3: P-selectin is highly expressed in the bone metastatic niche. (a) Both high P-selectin expression and elevated megakaryocytes/platelets number are seen in the bone marrow surrounding the tumour. Red: RFP constitutively expressed by tumour cells. Yellow: P-selectin, magenta: CD41 and blue: nuclei (DAPI staining). Dashed line outlines the tumour. The area designated by a white rectangle is showed at higher magnification in panel B. Scale bar: 100 µm. (b) Platelets and megakaryocytes express high level of P-selectin. Yellow: P-selectin, magenta: CD41 and blue: nuclei (DAPI staining). Scale bar: 50 µm. (c) P-selectin is expressed at the bone marrow endothelium in the breast cancer bone metastatic environment. Yellow: P-selectin, green: endomucin (vascular endothelium) and blue: nuclei (DAPI staining). Scale bar: 50 µm. (d) P-selectin expression is higher around the tumour area than in the rest of the bone marrow. P-selectin expression was quantified from bone marrow sections of 7 mice per area of 100 µm² from the tumour. r = Pearson correlation coefficient. * $p \leq 0.05$, *** $p \leq 0.001$, **** $p \leq 0.0001$.

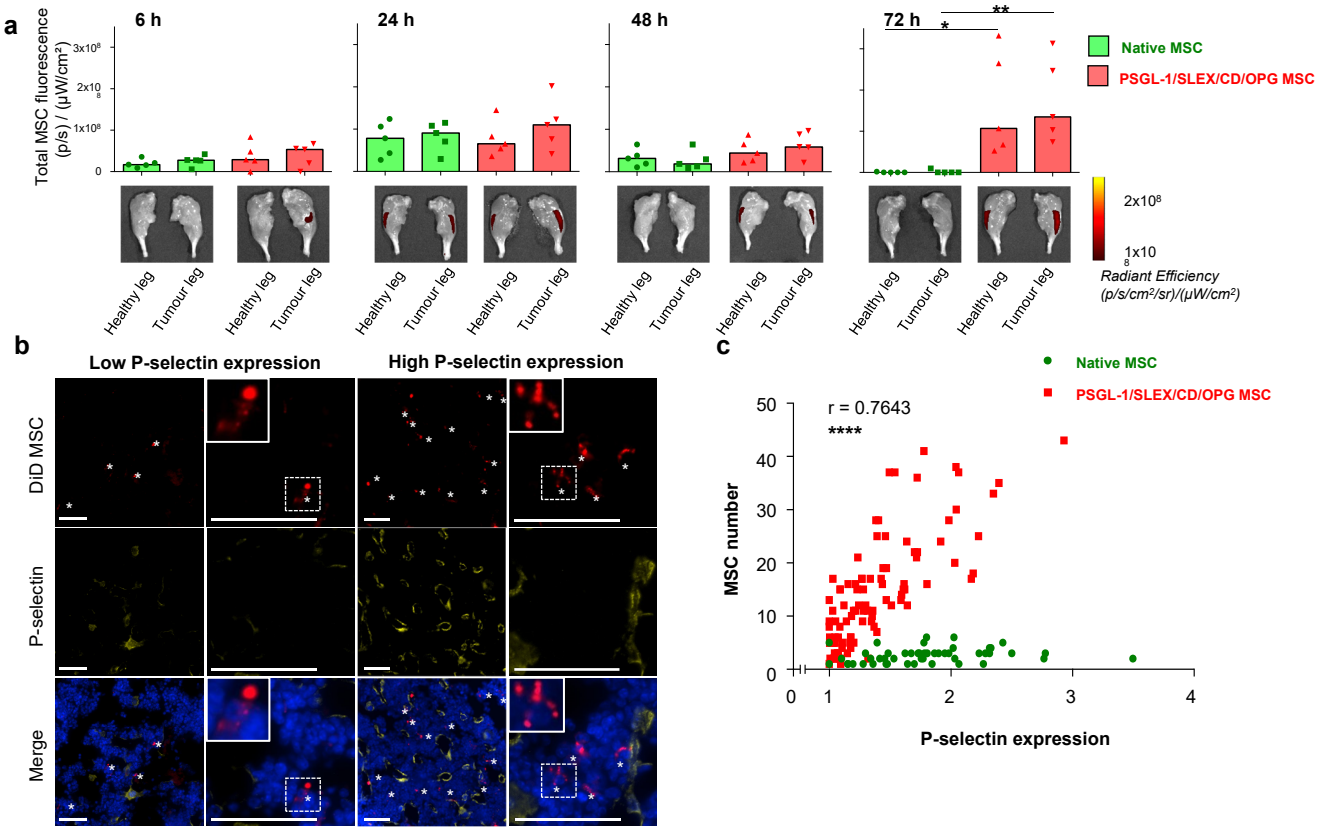

Figure 4: Enhanced homing of engineered MSC to breast cancer bone metastases *in vivo* in the MDA-MB231 intratibial model. (a) PSGL-1/SLEX/CD/OPG MSC display an increased homing to the tumour legs 72 hours post-transplantation. Native MSC or PSGL-1/SLEX/CD/OPG MSC labelled with DiD lipophilic dye were injected *i.v.*, then mice were euthanised at different time-points (6, 24, 48, and 72 hours). Homing to the legs was evaluated based on the fluorescence intensity of the DiD dye. Control animals that were not injected with MSC were used to subtract fluorescent background from true signal. Plot: median values, each point is an individual animal, n=5 animals per group, statistical analysis: Kruskal-Wallis with Dunn's multiple comparison test * $p \leq 0.05$ between Native MSC (healthy leg) and PSGL-1/SLEX/CD/OPG MSC (healthy leg), ** $p \leq 0.01$ between Native MSC (tumour leg) and PSGL-1/SLEX/CD/OPG MSC (tumour leg). (b) PSGL-1/SLEX/CD/OPG MSC accumulate in high P-selectin expression areas in the bone marrow section (48h post-transplantation time-point). Red: DiD stained MSC, yellow: P-selectin, blue: nuclei (DAPI staining). White stars designate MSC. Scale bars: 50 µm. (c) PSGL-1/SLEX/CD/OPG MSC number within the bone marrow is positively correlated to P-selectin expression. 200 µm by 200 µm areas containing MSC were selected for quantification from the 72 h time-point post-MSC transplantation. Average P-selectin signal was measured by dividing total photon counts emitted in Cy5 per surface area and subtracting the background signal. 49 areas were evaluated for Native MSC, and 95 areas were assessed for PSGL-1/SLEX/CD/OPG MSC. Statistical analysis: Pearson correlation test, coefficient r=0.7643, **** $p \leq 0.0001$ for PSGL-1/SLEX/CD/OPG MSC.

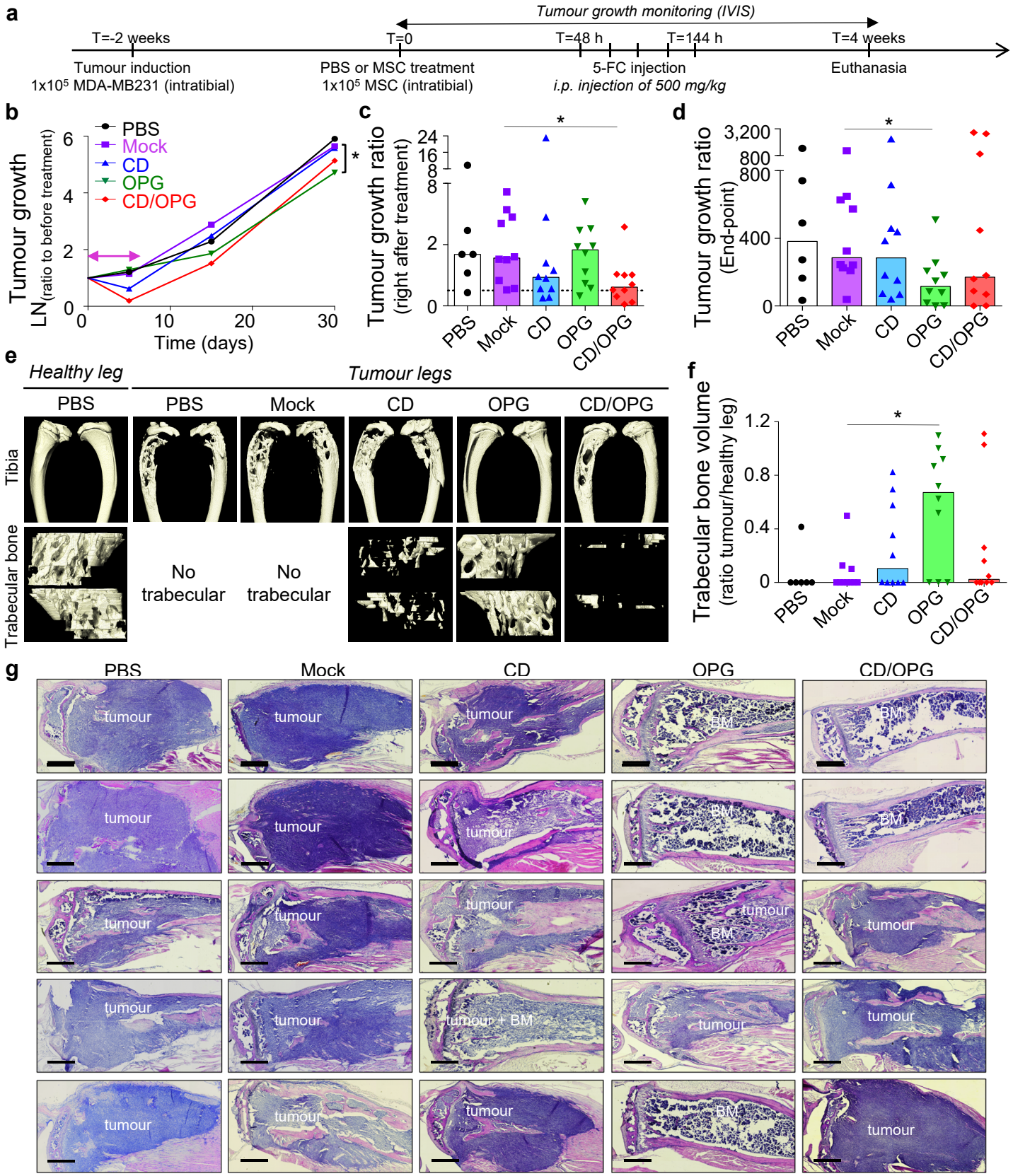

Figure 5: Engineered MSC exhibit therapeutic effects in treating bone metastases *in vivo* in the MDA-MB231 intratibial model. (a) Timeline of the therapeutic treatment validation. MSC were engineered as follows: Mock group (Mock transfected), CD group (PSGL-1/SLEX/CD), OPG group (PSGL-1/SLEX/OPG) and CD/OPG group (PSGL-1/SLEX/CD/OPG) and injected directly into the tibia, n=10 per group. PBS group only received PBS in the tibia instead of MSC, n=6. (b) The logarithm values of the tumour growth ratio (Total photon flux measured/Total photon flux on the day before the treatment started) are plotted over time for each group. Median of each group is shown. Pink double-headed arrow shows treatment duration. Statistical analysis: Kruskal-Wallis with Dunn's multiple comparison *post hoc*, * $p \leq 0.05$ between Mock MSC and OPG MSC. (c) Bar graph shows the tumour growth ratio measured on the day after the treatment is done. Each point represents one animal, and the bars represent the median value of the group. Dashed line indicates a tumour growth ratio of 1 (animals below that line have tumour decrease). Statistical analysis: Kruskal-Wallis with Dunn's multiple comparison *post hoc*, * $p \leq 0.05$ between Mock MSC and CD/OPG MSC. (d) Bar graph shows the tumour growth ratio measured on the end-point day. Each point represents one animal, and the bars represent the median value of the group. Statistical analysis: Kruskal-Wallis with Dunn's multiple comparison *post hoc*, * $p \leq 0.05$ between Mock MSC and OPG MSC. (e) MicroCT imaging was done on mouse tibias after euthanasia. Representative 3D reconstructions matching the median of each group for bone analysis are shown. First row shows whole tibias without the fibula, while bottom row shows trabecular bone. (f) Bar graph shows the trabecular bone ratio measured by normalising the trabecular bone volume of each tumour leg to the trabecular bone volume of healthy legs. Each point represents one animal, and the bars represent the median value of the group. Statistical analysis: Kruskal-Wallis with Dunn's multiple comparison *post hoc*, * $p \leq 0.05$ between Mock MSC and OPG MSC. (g) H&E staining of mouse tibias at end-point demonstrate treatment with OPG MSC and CD/OPG MSC can clear tumour cells and preserve the bone structure, while tumour invades the cortical bone in control animals (PBS and Mock MSC groups). 5 representative mouse tibias are shown for each group. BM=healthy bone marrow. Scale bar: 500 µm.

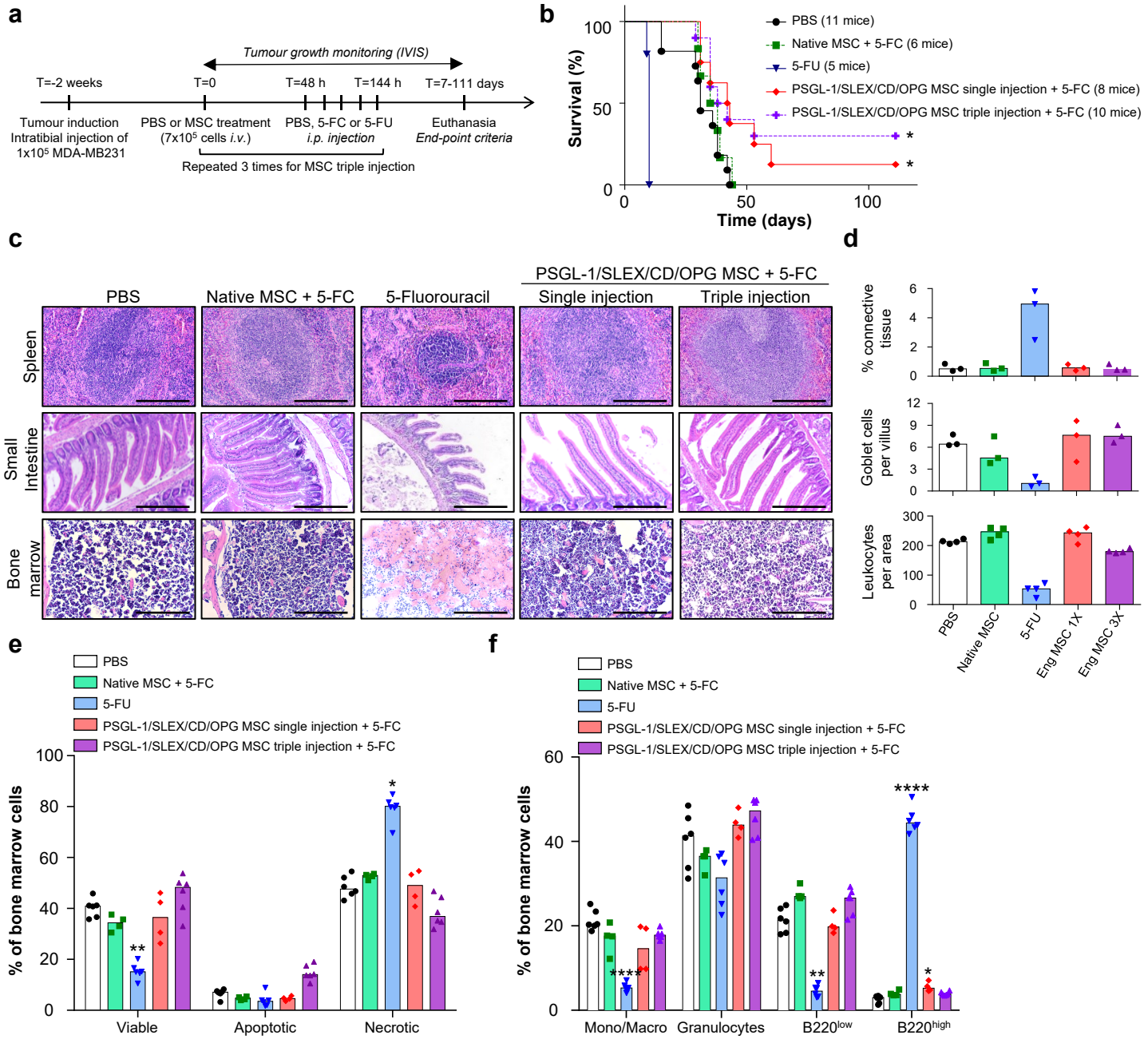

Figure 6: Systemic infusion of PSGL-1/SLEX/CD/OPG MSC improves animal survival without inducing systemic toxicity in the MDA-MB231 intratibial model.

(a) Timeline of the therapeutic treatments. PBS or 7x10^5 MSC (Native or PSGL-1/SLEX/CD/OPG) were injected *i.v.* and 48 hours later 500 mg/kg 5-FC or 200 mg/kg 5-FU was injected *i.p.* once a day for 5 days. Mice were euthanised as defined by end-point criteria (total photon flux >10^{10} p/s, signs of pain or distress, *etc.*). (b) PSGL-1/SLEX/CD/OPG MSC treatment improves overall animal survival. The graph shows the percentage of survival of the animals in the different groups: CT (PBS control, 11 mice), Native MSC + 5-FC treatment (6 mice), 5-FU (5 mice), PSGL-1/SLEX/CD/OPG MSC single injection + 5-FC treatment (8 mice) and PSGL-1/SLEX/CD/OPG MSC triple injection + 5-FC treatment (10 mice). Statistical analysis: Log-rank (Mantel-Cox) test, * $p \leq 0.05$. (c) PSGL-1/SLEX/CD/OPG MSC treatment group exhibits minimal systemic toxicity compared to 5-FU treatment. Tissue analysis was performed following H&E staining to evaluate toxicity-induced damage. Panel shows organs where the greatest damage was observed: spleen, small intestine, and bone marrow. Scale bars: 500 µm for spleen and bone marrow, 250 µm for the small intestine. (d) Engineered MSC did not induce significant tissue damage. Quantifications were done on the H&E staining: percentage of connective tissue to assess of spleen fibrosis, number of goblet cells per villus to evaluate intestine damage, and number of leukocytes per bone marrow area to measure toxicity. Bar graph shows the median for each group, and each point represents one animal, n=4 mice per group. Eng MSC = PSGL-1/SLEX/CD/OPG MSC. (e) Engineered MSC did not lead to significant cell death in the bone marrow. Flow cytometry was performed on bone marrow to analyze the percentages of viable, apoptotic and necrotic cells. 2 to 3 animals were used for each group, and both legs were analysed. As no major differences were observed between the healthy and the tumour leg, data from both legs were pooled. Bar graph shows the median for each group, and each point represents one analysed leg. Statistical analysis: Kruskal-Wallis followed by a Dunn's multiple comparison test among each group (viable, apoptotic and necrotic) to compare all conditions to the control; * $p \leq 0.05$, ** $p \leq 0.01$. (f) Engineered MSC did not significantly alter cell composition of the bone marrow. Flow cytometry was performed on equal numbers of bone marrow cells to analyze the different populations: monocytes/macrophages (Mono/Macro), granulocytes and B lymphocytes (B220^{low} and B220^{high}). 2 to 3 animals were used for each group, and both legs were analysed. As no major differences were observed between the healthy and the tumour leg, data from both legs were pooled. Bar graph shows the median for each group, and each point represents one analysed leg. Statistical analysis: Kruskal-Wallis followed by a Dunn's multiple comparison test among each population to compare all conditions to the control; * $p \leq 0.05$, **** $p \leq 0.0001$.

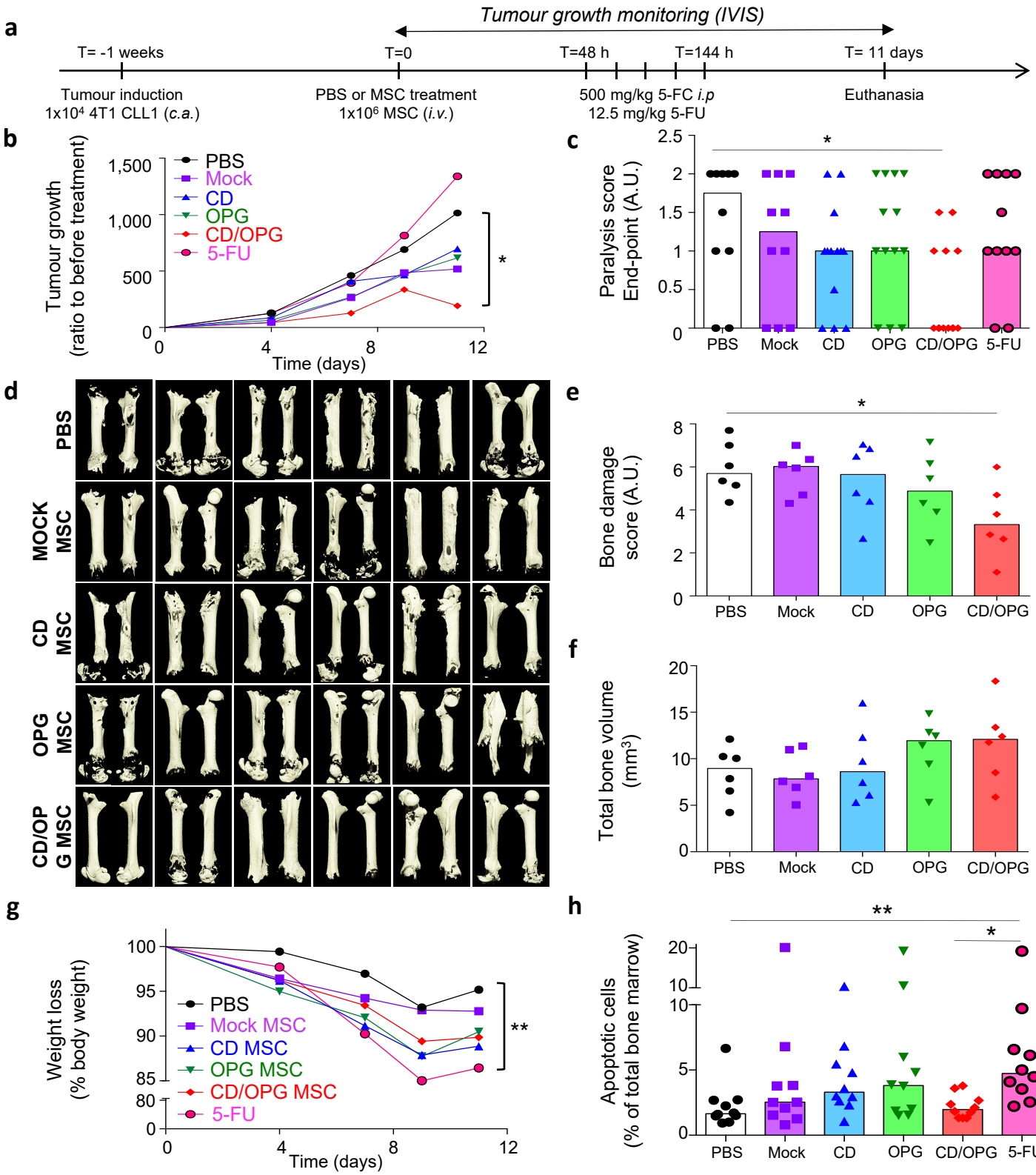

Figure 7: CD/OPG MSC exhibit therapeutic effects and minimal toxicity in a syngeneic mouse model of spontaneous bone metastases. (a) Timeline of the therapeutic treatment. Spontaneous bone metastases were induced by caudal artery injection of a 4T1 bone metastatic clone (CLL1) to BALB/cJ mice. Once bone metastases were detected, engineered MSC or PBS were systemically administered to animals via *i.v.* injection, and 5-FC was injected *i.p.* for 5 consecutive days 48 h post transplantation. 12.5 mg/kg 5-FU was used as a reference group for treatment. MSC were engineered as follows: Mock group (Mock transfected), CD group (PSGL-1/SLEX/CD), OPG group (PSGL-1/SLEX/OPG) and CD/OPG group (PSGL-1/SLEX/CD/OPG). PBS, Mock and 5-FU groups: n=10 animals per group. CD, OPG and CD/OPG groups: n=13 per group. (b) CD/OPG MSC inhibits tumour growth compared to PBS control group. Bioluminescence imaging was performed over time and signal was quantified in the lower body to measure bone metastases development in legs and spine. The median of the tumour growth ratio (total photon flux over time normalised to total photon flux before treatment) was plotted for each group. Statistical analysis done at the end-point: Kruskal-Wallis with Dunn's multiple comparison post hoc, * $p \leq 0.05$ between PBS and CD/OPG MSC. (c) CD/OPG treatment improved mouse mobility. Paralysis of the animals was scored at the end-point (see Methods). Bar graph shows the median score for each group, and each point represents one animal. Statistical analysis: Kruskal-Wallis with Dunn's multiple comparison post hoc, * $p \leq 0.05$ between PBS and CD/OPG MSC. (d) Femurs bearing bone metastases are less damaged in CD/OPG MSC treated group. Micro-CT analysis was done on mouse femurs exhibiting clear leg metastases (usually around the hip area) before treatment from 6 mice per group. 3D reconstructions were made from the whole femurs. (e) Bone damage was blindly scored by a panel of 20 unbiased persons (shaft damage from 0-3 and epiphysis damage from 0-5 based on importance of damage). The average scoring was shown for each animal. Bar graph represents the median score for each group, and each point represents one animal. Statistical analysis: Kruskal-Wallis with Dunn's multiple comparison post hoc, * $p \leq 0.05$ between PBS and CD/OPG MSC. (f) CD/OPG MSC and OPG MSC treatments seem to protect against bone loss. The total bone volume was quantified for each femur. Bar graph shows the median bone volume for each group, and each point represents one animal. Statistical analysis: Kruskal-Wallis with Dunn's multiple comparison post hoc. (g) 5-FU treatment, but not MSC groups, induces significant body weight loss. Graph shows the median body weight loss for each group over time. Statistical analysis done at the end-point: Kruskal-Wallis with Dunn's multiple comparison post hoc, ** $p \leq 0.01$ between PBS and 5-FU. (h) Only 5-FU treatment induces additional apoptosis in the bone marrow. At the end-point, the bone marrow of the healthier leg was isolated and cell apoptosis was analysed using flow-cytometry (AnnexinV+/7-AAD-) for n=10 animals per group. Bar graph shows the median percent of apoptosis for each group, and each point represents one animal. Statistical analysis: Kruskal-Wallis with Dunn's multiple comparison post hoc, * $p \leq 0.05$ between 5-FU and CD/OPG MSC, and ** $p \leq 0.01$ between PBS and 5-FU.

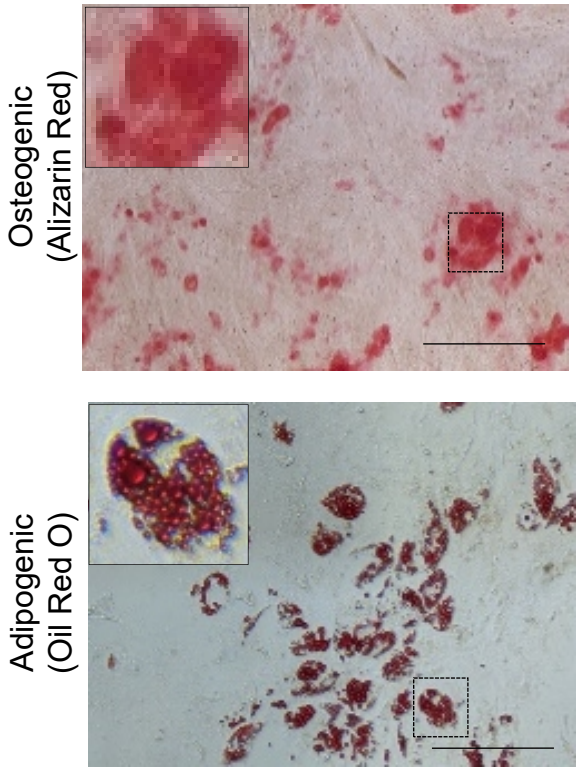

Supplementary Figure 1: PSGL-1/SLEX/CD/OPG MSC conserve their differentiation abilities after mRNA engineering. 24 h post mRNA engineering, PSGL-1/SLEX/CD/OPG MSC were plated to confluence and treated for osteogenic and adipogenic differentiation for 2-3 weeks. Image in the upper left corner shows a higher magnification of the area selected by the dashed line square in the larger image. Alizarin Red: calcium staining, Oil Red O: lipids staining. Scale bar: 250 µm.

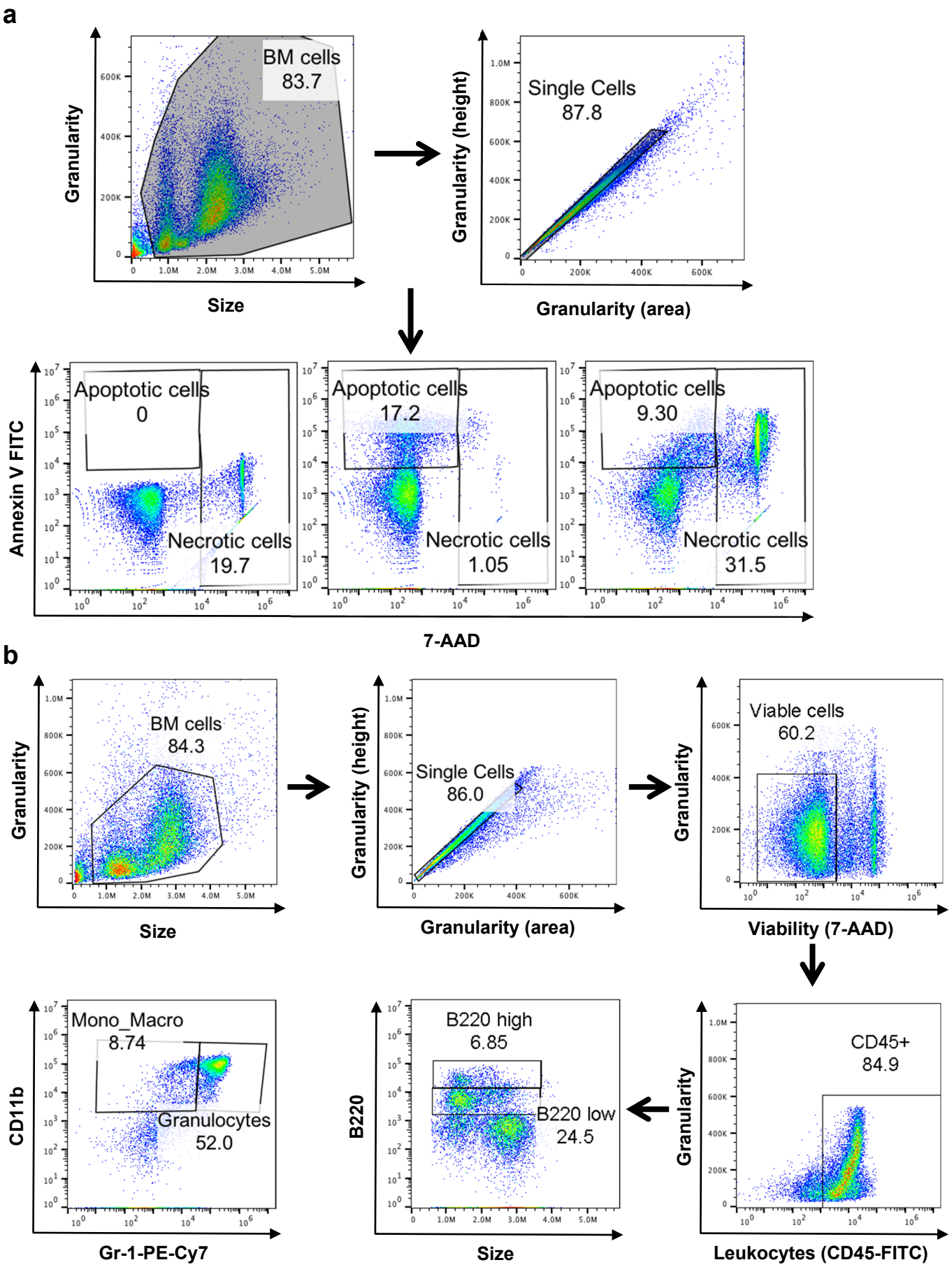

Supplementary Figure 2: Example of gating strategies used to analyze bone marrow cells. (a) Apoptotic cells and necrotic cells were analysed using 7-AAD and Annexin V FITC. After gating bone marrow cells based on size and granularity, single cells were selected, then apoptotic gate (Annexin $V^+/7\text{-}AAD^-$) and necrotic gate (Annexin $V^-/7\text{-}AAD^+$) were drawn from single stains. (b) Different cell populations were analysed in the bone marrow. First, bone marrow cells were selected based on their size and granularity, then single cells were selected. Within the viable cells ($7\text{-}AAD^-$), leukocytes ($CD45^+$) were selected to remove erythrocytes which did not get lysed. Finally, B cells ($B220^{low\ or\ high}$), monocytes/macrophages ($CD11b^+/Gr\text{-}1^{neg\ or\ low}$), and granulocytes ($CD11b^+/Gr\text{-}1^{high}$) were quantified.

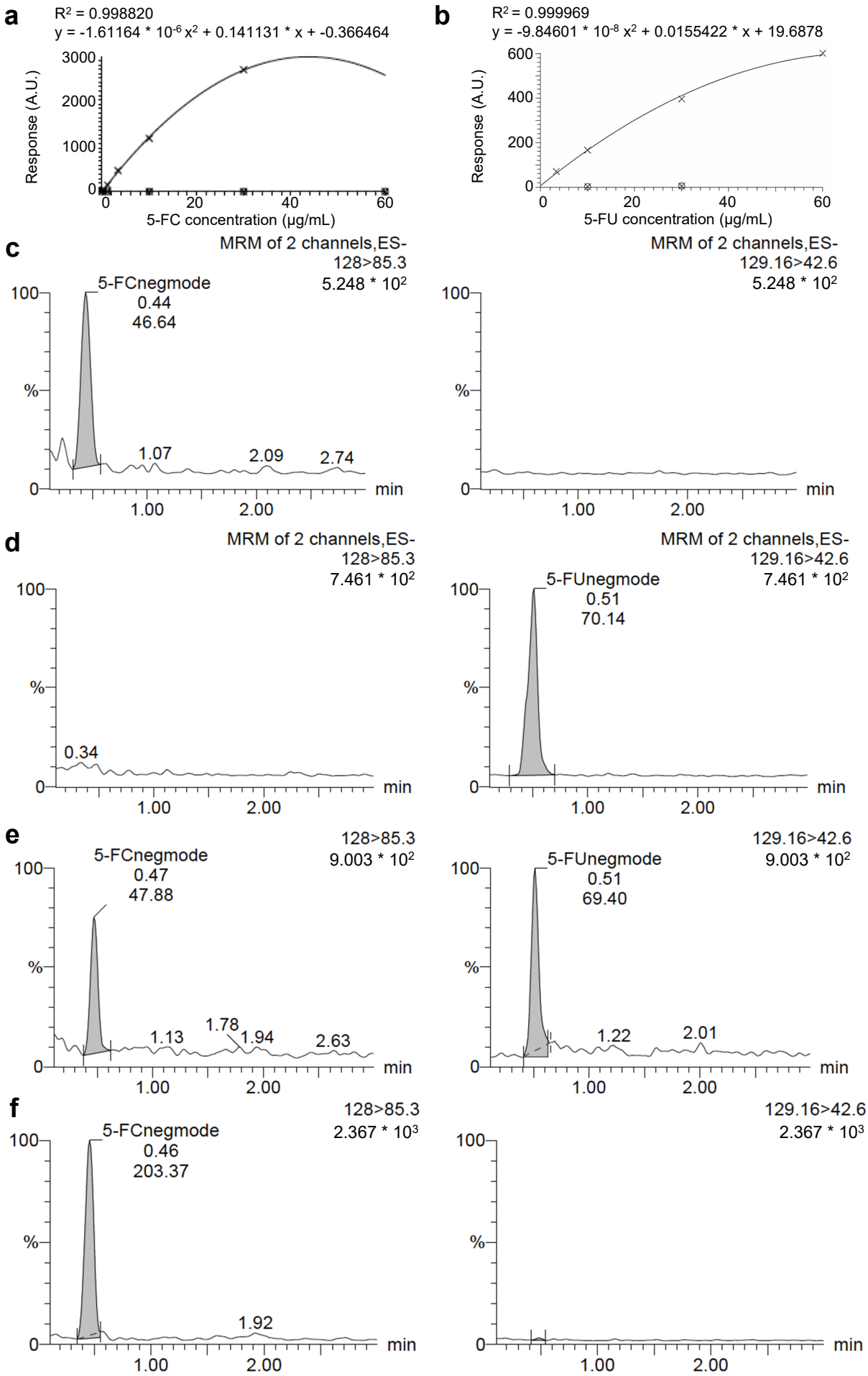

Supplementary Figure 3: The conversion of 5-Fluorocytosine (5-FC) pro-drug into 5-Fluorouracil (5-FU) by PSGL-1/SLEX/CD/OPG MSC were measured by mass spectrometry. (a) A standard curve was determined from serial dilutions of 5-FC in water using negative ion mode (ES-). (b) A standard curve was determined from serial dilutions of 5-FU in analysis buffer using negative ion mode (ES-). (c) 370 ng/mL of 5-FC was easily detectable using m/z 128>85 specific transition for 5-FC, while nothing was detected using m/z 129>42 specific transition for 5-FU. (d) 3,300 ng/mL of 5-FU was easily detectable using m/z 129>42 specific transition for 5-FU while nothing was detected using m/z 128>85 specific transition for 5-FC. (e) 5-FC and 5-FU compounds were detected in conditioned medium of 100,000 PSGL-1/SLEX/CD/OPG MSC plated in presence of 400 µg/mL 5-FC after 1 day of culture. (f) 5-FC but no 5-FU compound was detected in conditioned medium of 100,000 Mock MSC plated in presence of 400 µg/mL 5-FC after 1 day of culture.

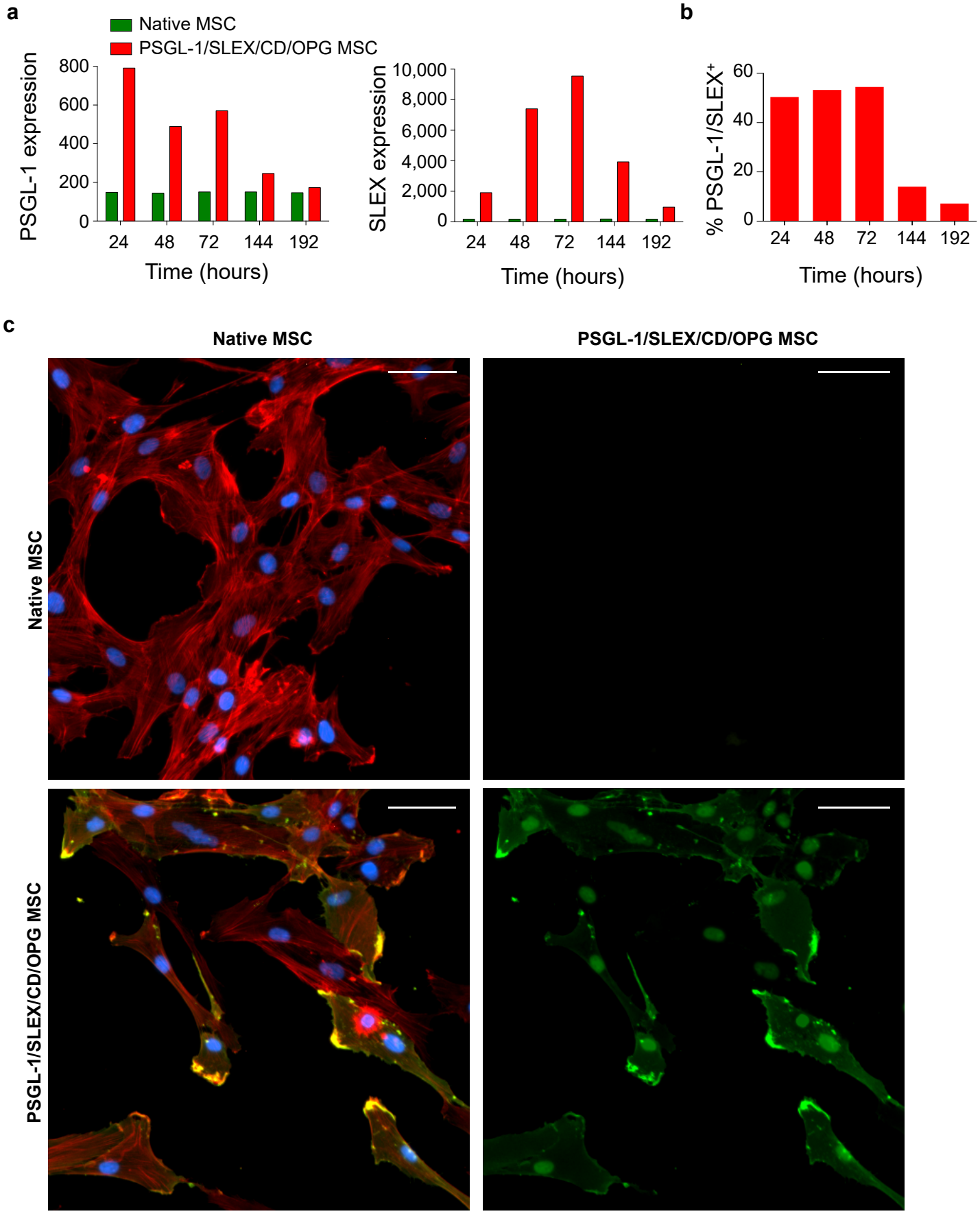

Supplementary Figure 4: *In vitro* functional validation of PSGL-1/SLEX expression by engineered MSC. (a) PSGL-1/SLEX/CD/OPG MSC expressed PSGL-1 and SLEX up to 6 days at the cell membrane. Flow cytometry was done on Native MSC and PSGL-1/SLEX/CD/OPG MSC at days 1, 2, 3, 6, and 8 to measure PSGL-1 and SLEX expression at the cell surface. Histograms show the median of fluorescence (MFI) for SLEX expression (FL-1) and PSGL-1 expression (FL-2). (b) Approximately 50% of engineered MSC expressed both PSGL-1 and SLEX over 3 days post-transfection. Percent of double positive cells for PSGL-1 and SLEX was analysed by flow cytometry. Histogram shows percentages of double positive MSC for PSGL-1 and SLEX. (c) PSGL-1 was localised at the pseudopodia of PSGL-1/SLEX/CD/OPG MSC. Immunofluorescence staining was done against PSGL-1 on Native MSC and PSGL-1/SLEX/CD/OPG MSC 24 h post-engineering. Green: PSGL-1, red: F-Actin (Phalloidin 594 nm) and blue: nuclei (DAPI staining). Scale bar: 100 µm.

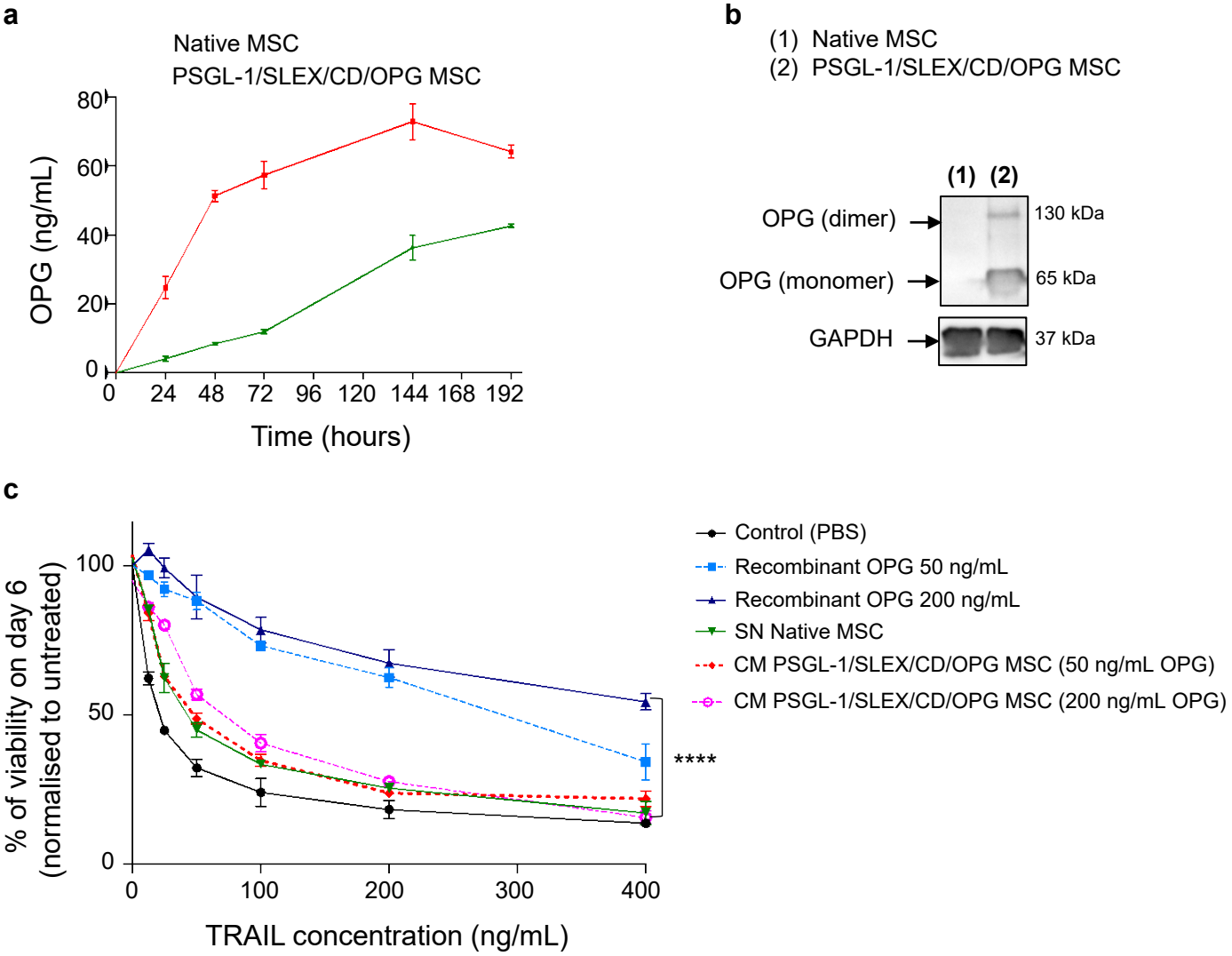

Supplementary Figure 5: *In vitro* functional validation of OPG secreted by engineered MSC. (a) PSGL-1/SLEX/CD/OPG MSC secrete soluble form of human OPG. ELISA was performed on conditioned media from Native MSC and PSGL-1/SLEX/CD/OPG MSC cultured for 8 days to measure secreted OPG (Native and engineered forms). Graph shows mean ± SD. (b) PSGL-1/SLEX/CD/OPG MSC express truncated OPG fused to Fc fragment from human IgG1. Western blot was performed on cell lysates at 24 h post-engineering against human Fc fragment. GAPDH was used as a loading control. (c) Recombinant human osteoprotegerin inhibits TRAIL apoptotic activity whereas the engineered form of OPG secreted by PSGL-1/SLEX/CD/OPG MSC does not. Viability of MDA-MB231 cells was determined in presence of increasing concentrations of TRAIL and recombinant human osteoprotegerin or concentrated conditioned media of Native and PSGL-1/SLEX/CD/OPG MSC (10 µL of PSGL-1/SLEX/CD/OPG MSC concentrated supernatant is equivalent to 50 ng/mL and 40 µL is equivalent to 200 ng/mL as previously determined by ELISA). Viability assay was performed 24 h after treatment using Alamar blue assay. Graph shows mean ± SD. ****$p \leq 0.0001$ between recombinant OPG 200 ng/mL and CM PSGL-1/SLEX/CD/OPG MSC (200 ng/mL OPG) using unpaired *t* test.

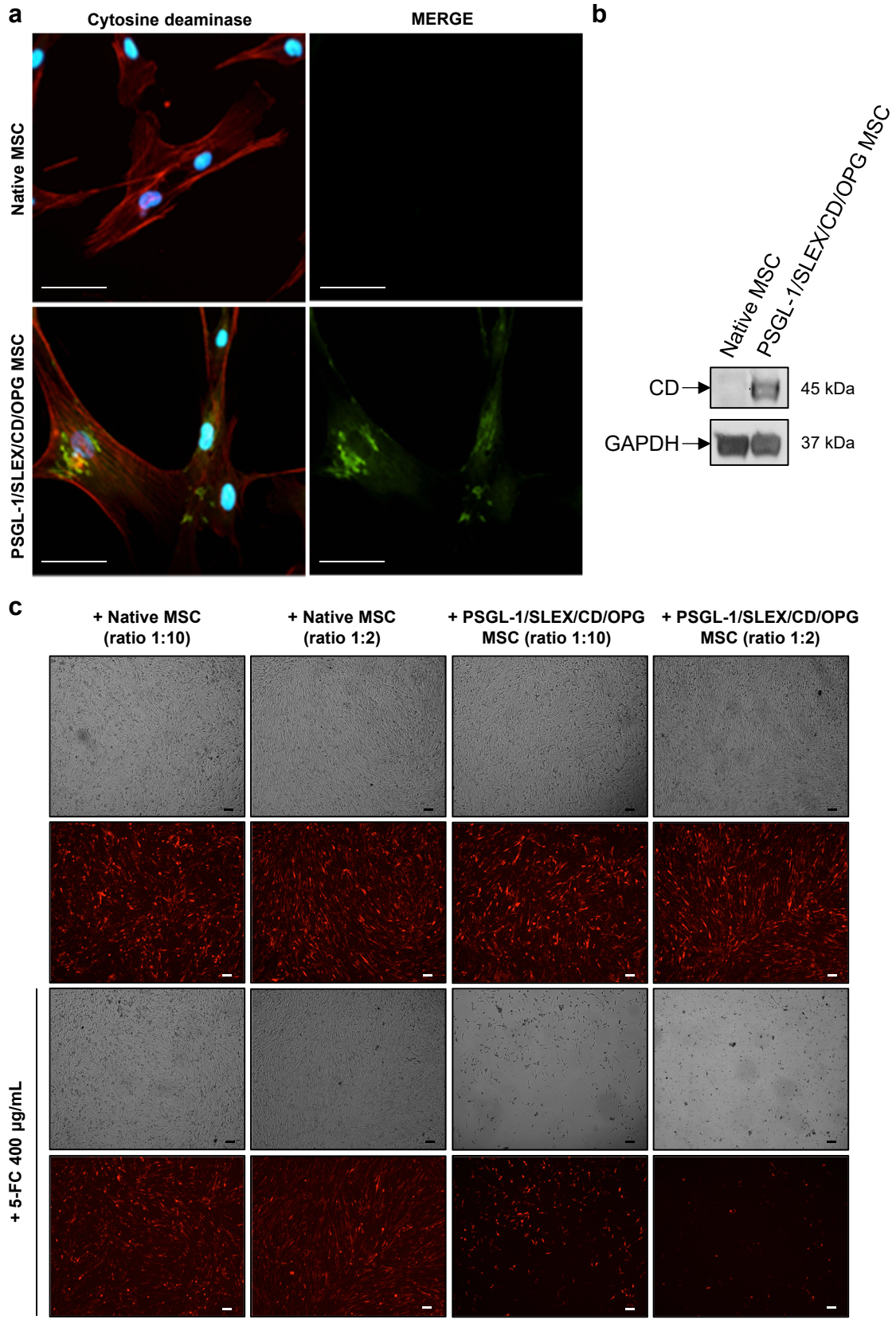

Supplementary Figure 6: *In vitro* functional validation of CD expression by engineered MSC. (a) PSGL-1/SLEX/CD/OPG MSC showed intracellular expression of CD. Immunofluorescence was done on Native and PSGL-1/SLEX/CD/OPG MSC at 24 h post-engineering. Green: CD, red: phalloidin, and blue: nuclei (DAPI staining). Scale bar: 100 µm. (b) The molecular weight of the CD expressed by PSGL-1/SLEX/CD/OPG MSC matched the molecular weight of the original protein (CD fused to uracil phosphoribosyltransferase). Western blot against CD was performed on cell lysates at 24 h post-engineering. GAPDH was used as a loading control. (c) PSGL-1/SLEX/CD/OPG MSC killed cancer cells when co-cultured in presence of 5-Fluorocytosine. Pictures show the co-cultures at day 6; brightfield shows both cell types in direct co-culture, whereas fluorescent images only show MDA-MB231 expressing RFP (red). Scale bar: 100 µm.

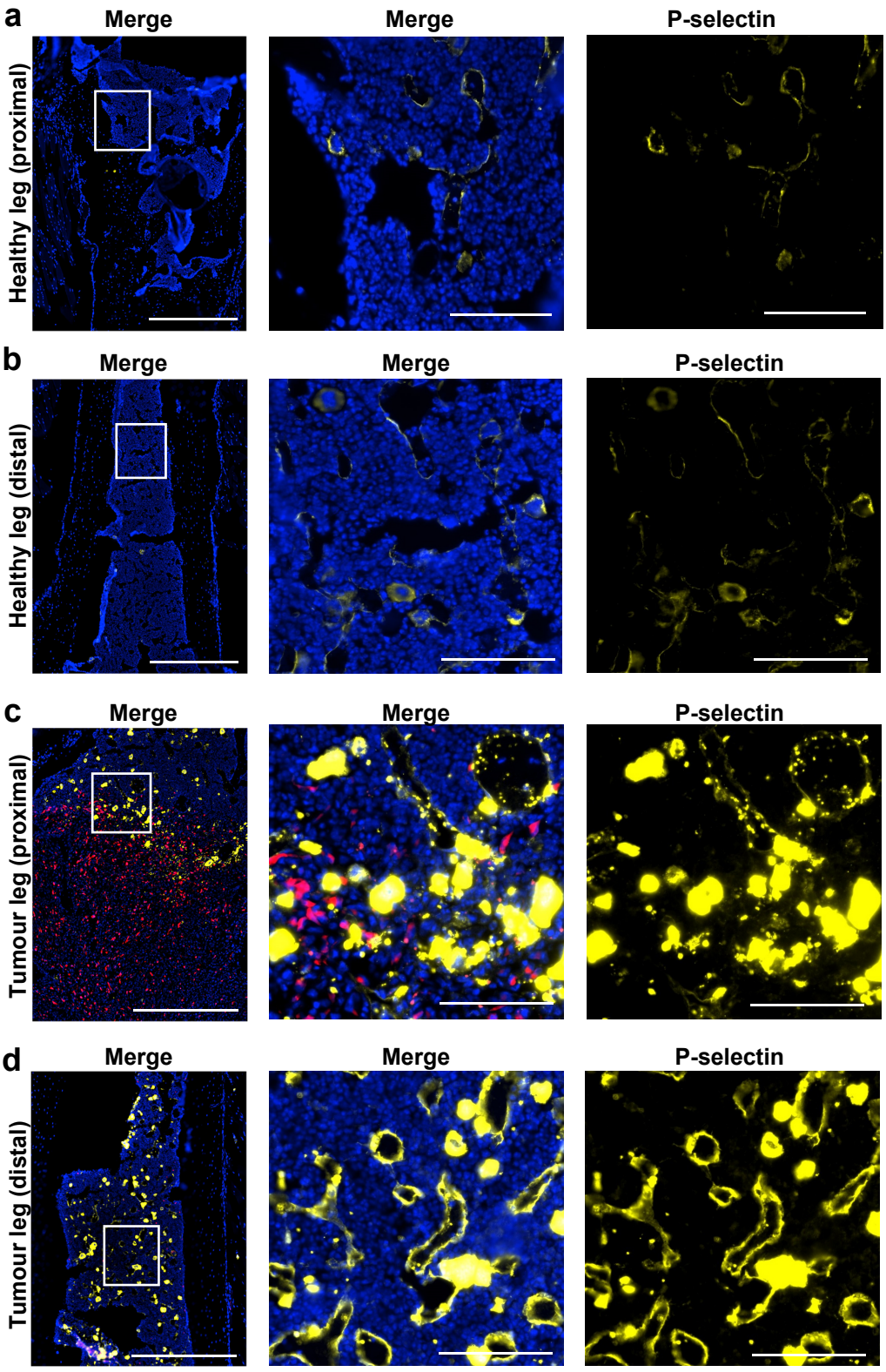

Supplementary Figure 7: P-selectin expression within the bone marrow was increased around the tumour area. Panels a to d show bone marrow sections from the healthy tibia and tumour bearing tibia from the same mouse sectioned, stained, and imaged side by side. The two images on the right are higher magnifications of the area delimited by a white rectangle on the left image. Red: RFP constitutively expressed by tumour cells, yellow: P-selectin, blue: nuclei (DAPI staining). Scale bar is 5,000 µm for the left merge image, and 100 µm for the two higher magnification images on the right. (a) Proximal extremity of the tibia section of the healthy leg. (b) Distal extremity of the tibia section of the healthy leg. (c) Proximal extremity of the tibia section of the tumour leg. (d) Distal extremity of the tibia section of the tumour leg.

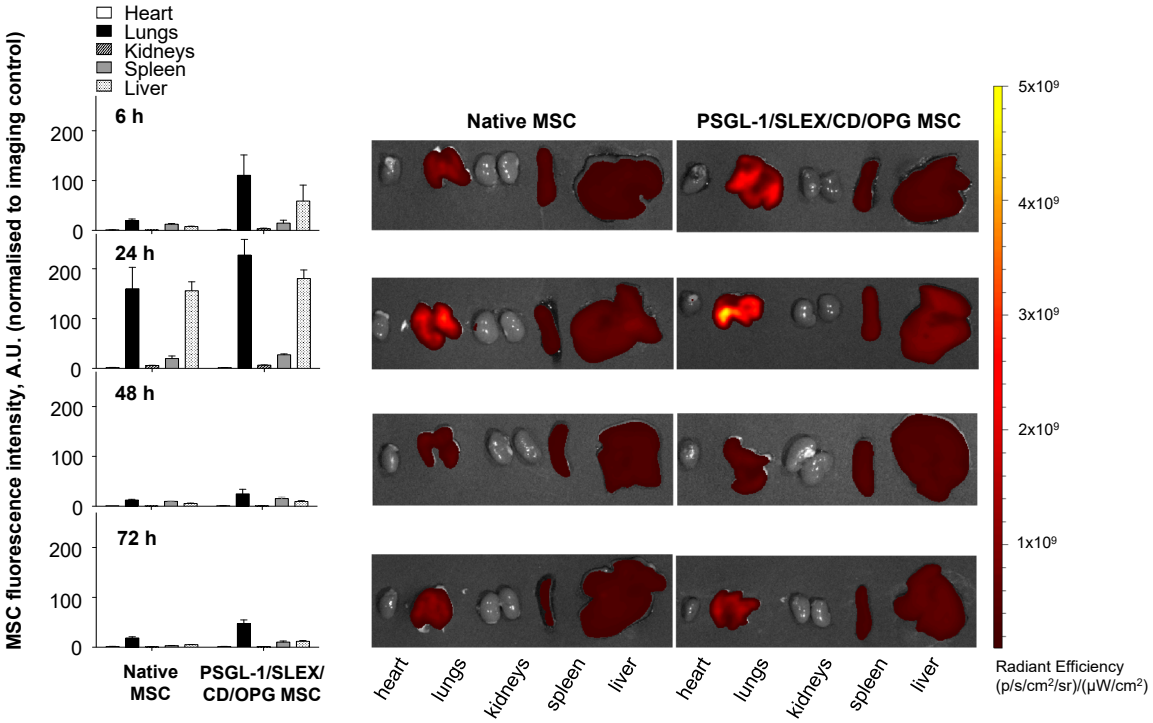

Supplementary Figure 8: MSC entrapped into the lungs following *i.v.* injection, in the MDA-MB231 intratibial model, were mostly cleared out by 48 hours post-transplantation. Native or PSGL-1/SLEX/CD/OPG MSC labelled with DiD lipophilic dye were injected *i.v.* and mice were euthanised at different time-points (6, 24, 48, and 72 h) to harvest the different organs. MSC signal in the heart, lungs, kidneys, spleen, and liver was measured using fluorescence intensity. Control mice without MSC injection were used to normalise the data and discriminate fluorescent background from true signal.

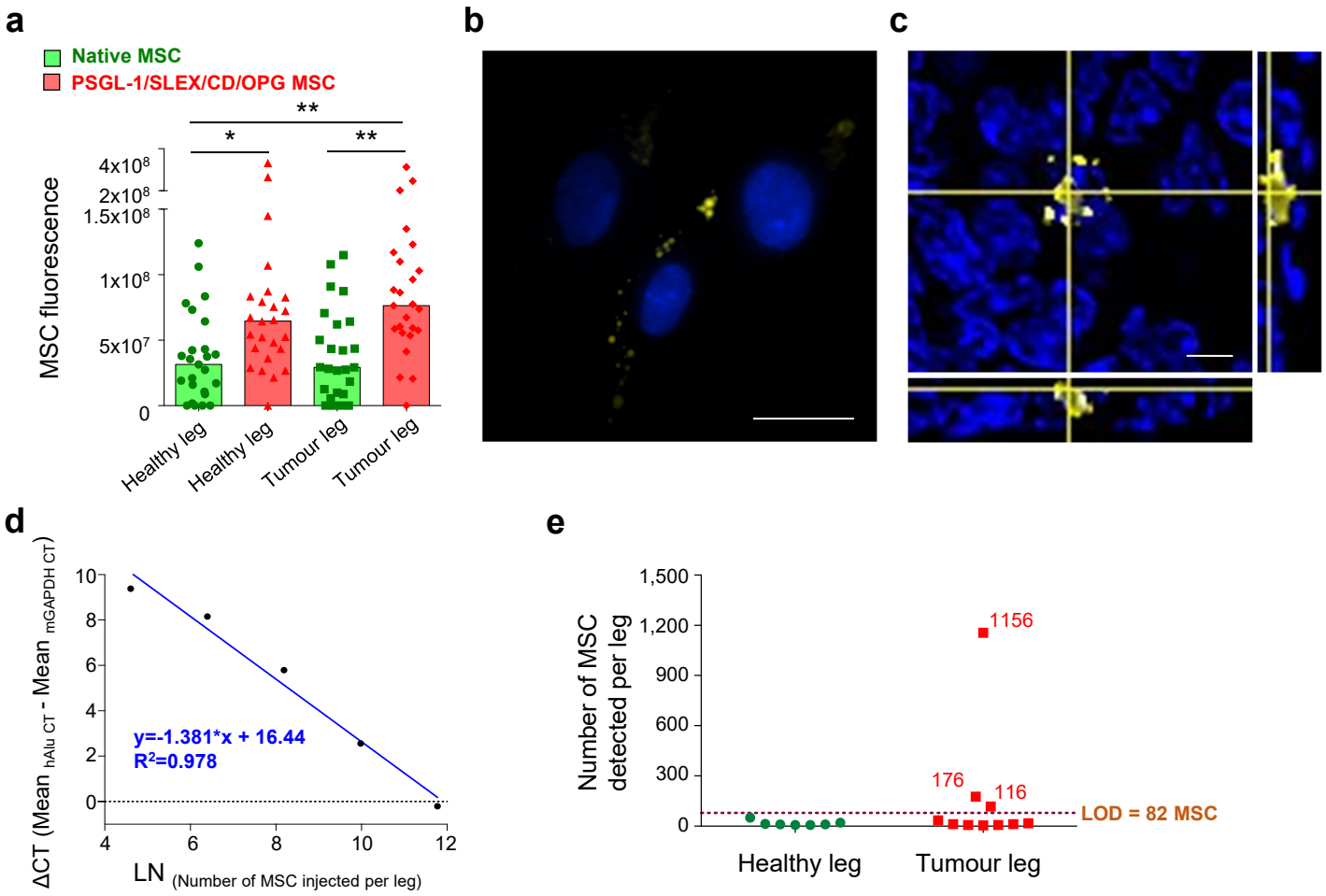

Supplementary Figure 9: PSGL-1/SLEX/CD/OPG MSC display more effective homing than Native MSC to the bone marrow, in particular to bone metastatic tumours, in the immunocompromised intratibial model (a-c) and in the syngeneic model of spontaneous bone metastasis (d,e). (a) Native MSC or PSGL-1/SLEX/CD/OPG MSC labelled with DiD lipophilic dye were injected *i.v.*, then mice were euthanised at different time-points (6, 24, 48, and 72 hours, and 1 week). Homing to the legs was evaluated based on the fluorescence intensity of the DiD dye. All time-points were combined together to compare overall homing to the healthy and to the tumour legs for Native MSC or PSGL-1/SLEX/CD/OPG MSC. Bar graph shows median values, and each point represents one animal at a specific time post-MSC transplantation. Statistical test: ANOVA with Turkey's multiple comparisons test, * $p \leq 0.05$ *and* ** $p \leq 0.01$. (b) Remaining PSGL-1/SLEX/CD/OPG MSC were put back in culture after cell transplantation to animals, and MSC were imaged 72 hours later, which shows DiD lipophilic dye persists several days post MSC labelling. Scale bar: 25 µm. (c) DiD stained PSGL-1/SLEX/CD/OPG MSC are seen in the bone marrow of transplanted animals 72 hours post-transplantation. Scale bar: 20 µm. (d) Human MSC can be detected in mouse legs of BALB/cJ using ALU qPCR (see Methods). (e) PSGL-1/SLEX/CD/OPG MSC are detected in tumour legs in a syngeneic model of bone metastasis, but not in healthy legs. 5 healthy BALB/cJ and 10 animals bearing bone metastasis in the legs (4T1 CLL1 model) were injected *i.v.* with PSGL-1/SLEX/CD/OPG MSC, and euthanised 72 hours post-transplantation to collect the legs. Healthy legs (n=7; 6 from healthy animals and 1 from a tumour animal) and tumour legs (n=10) were analysed. Graph shows MSC number detected for each animal, as well as the limit of detection (LOD) of our assay, as determined from the ΔCT value for the negative control minus 2 CT.

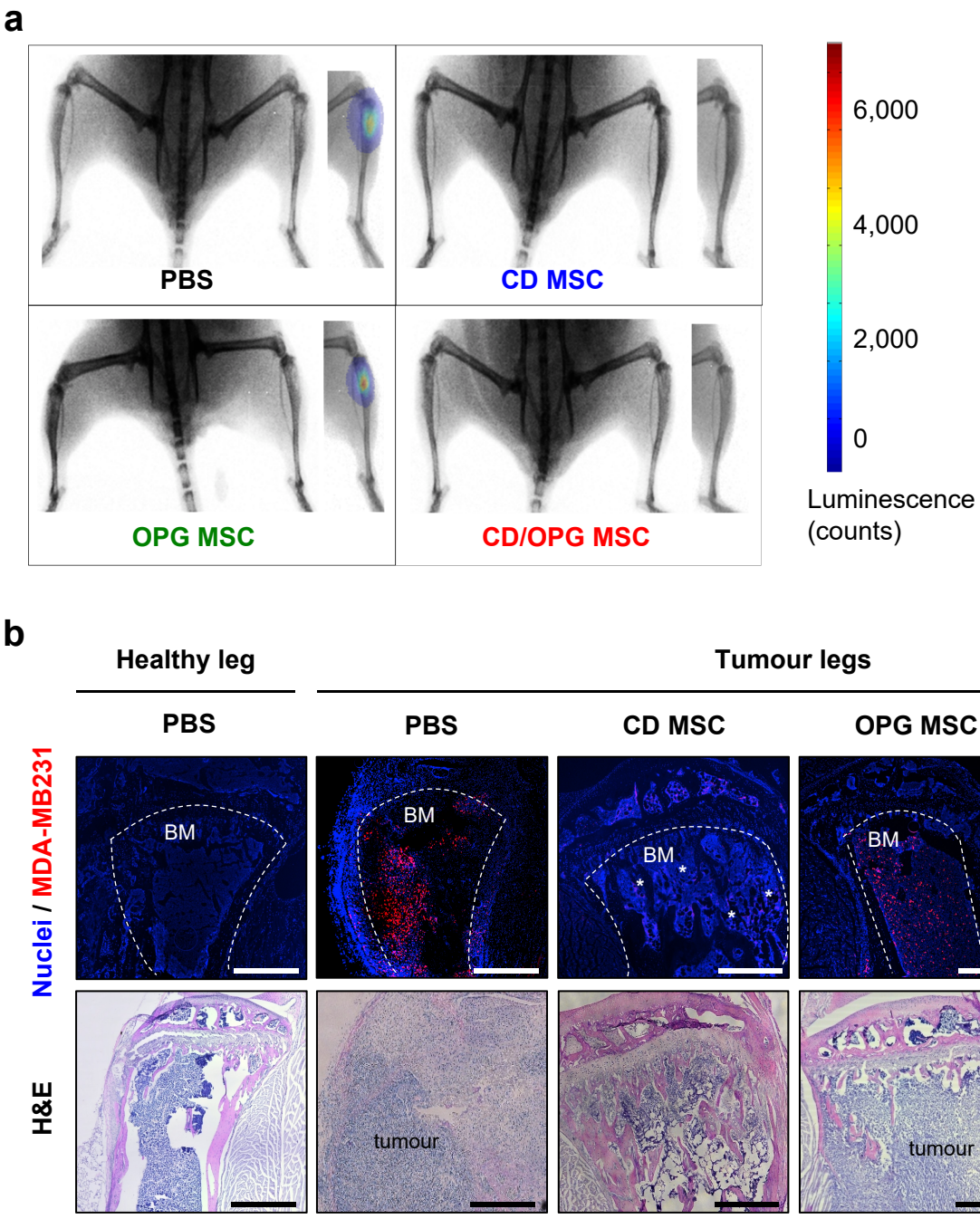

Supplementary Figure 10: Representative techniques to monitor and characterise engineered MSC's tumour killing efficacy in the MDA-MB231 intratibial model. (a) Representative combined *in vivo* X-ray imaging and bioluminescence imaging were used to confirm that breast tumours were growing within the bone marrow cavity of the tibias and to quickly assess tumour-induced bone damage. (b) Representative *ex vivo* analysis shows CD and CD/OPG MSC treatments injected directly into the tibia prevented tumour invasion within the bone marrow and cortical bone damages. Top panel shows DAPI staining (nuclei in blue) on representative tibia sections for each group. MDA-MB231 were localised using their RFP expression (red). BM: bone marrow cavity. *: residual RFP positive tumour cells not detected using IVIS imaging. Bottom panel shows corresponding H&E staining for each tibia sections (serial cuts). Scale bar: 500 µm.

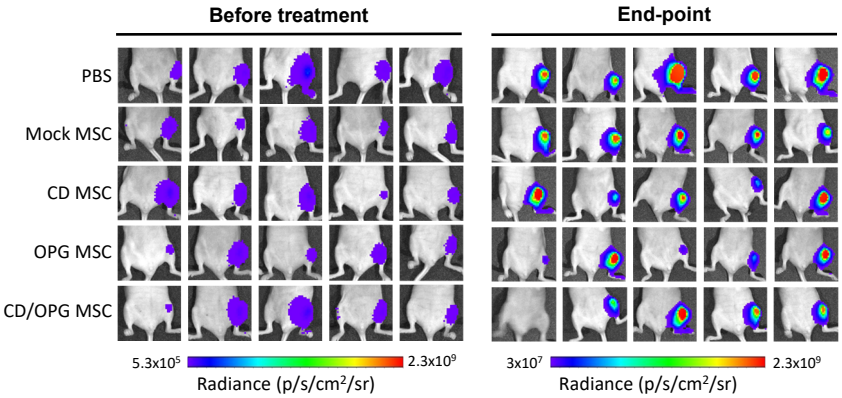

Supplementary Figure 11: Representative *in vivo* imaging data demonstrate the inhibition by engineered MSC treatment on MDA-MB231 tumour growth in the tibias of Nude mice in the MDA-MB231 intratibial immunocompromised model. Tumour growth within the tibia was monitored using bioluminescence imaging following transplantation of mock transfected MSC (Mock MSC group), PSGL-1/SLEX/CD MSC (CD MSC group), PSGL-1/SLEX/OPG MSC (OPG MSC group) or PSGL-1/SLEX/CD/OPG MSC (CD/OPG MSC group), all administered via an intratibial injection. Figure shows tumour signal before the treatment and at the end-point for 5 representative animals. Quantification of this study is presented in Figure 5.

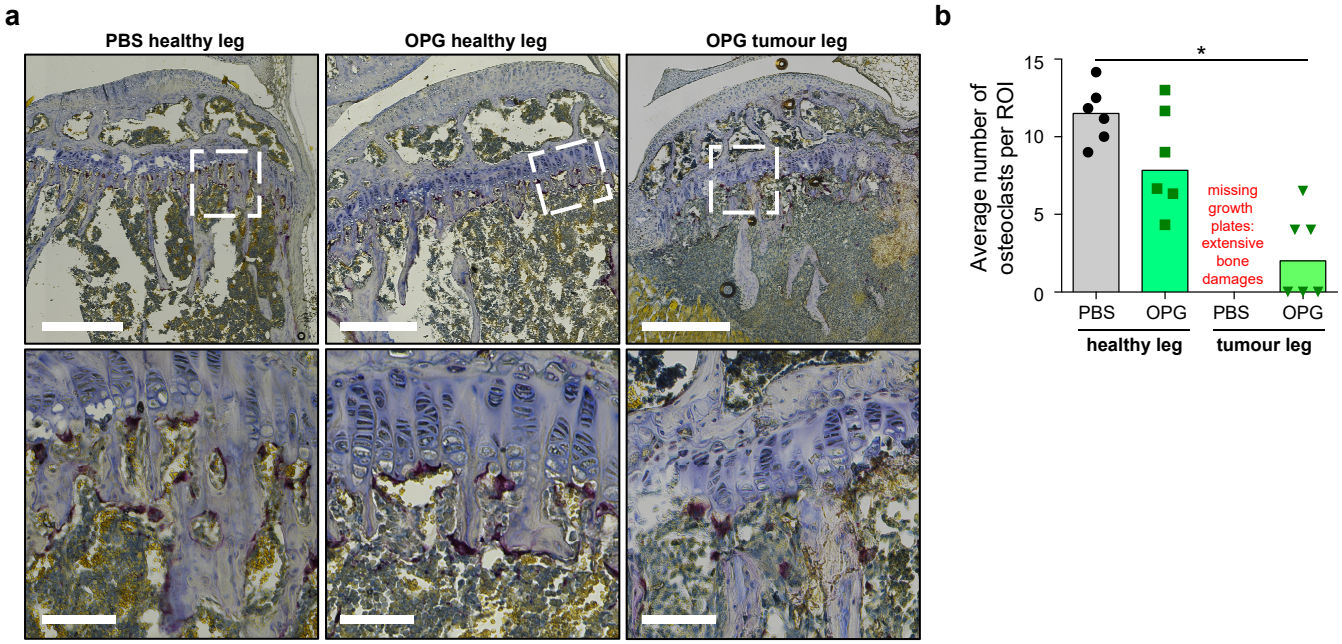

Supplementary Figure 12: PSGL-1/SLEX/OPG MSC inhibit tumour-induced osteoclast activity in the MDA-MB231 intratibial model, thus preventing bone loss. (a) OPG MSC treatment via intratibial injection reduced the density of TRAP$^+$ activated osteoclasts seen at the tibia epiphysis. TRAP staining followed by Hematoxylin counterstain was performed on several tibia sections from the healthy legs of control animals (PBS group), and the healthy legs and tumour legs of animals treated with PSGL-1/SLEX/OPG MSC (OPG group) injected directly into the tibia. Second row shows higher magnification of the selected ROI (white dashed line) from the images presented on the top panel. Scale bars: 500 µm for upper panel and 100 µm for lower panel. (b) The number of TRAP$^+$ activated osteoclasts was significantly lower in the tumour legs of mice treated with PSGL-1/SLEX/OPG MSC injected directly into the tibia. The average number of TRAP$^+$ osteoclasts was counted in a minimum of three ROIs per leg, distributed across the tibia growth plate, for each animal. Bar graph shows the average number of osteoclasts per ROI for each animal, n=6 per group. Each point represents one animal, and the bars represent the median value of the group. No analysis could be done on tumour legs of mice from the PBS group as the growth plate was destroyed by the tumour, indicating a strong osteoclast activity. PBS: PBS treated group, OPG group: PSGL-1/SLEX/OPG MSC treated group. Statistical analysis: Kruskal-Wallis with Dunn's multiple comparison *post hoc*, * $p \leq 0.05$ between PBS healthy legs and OPG MSC tumour legs.

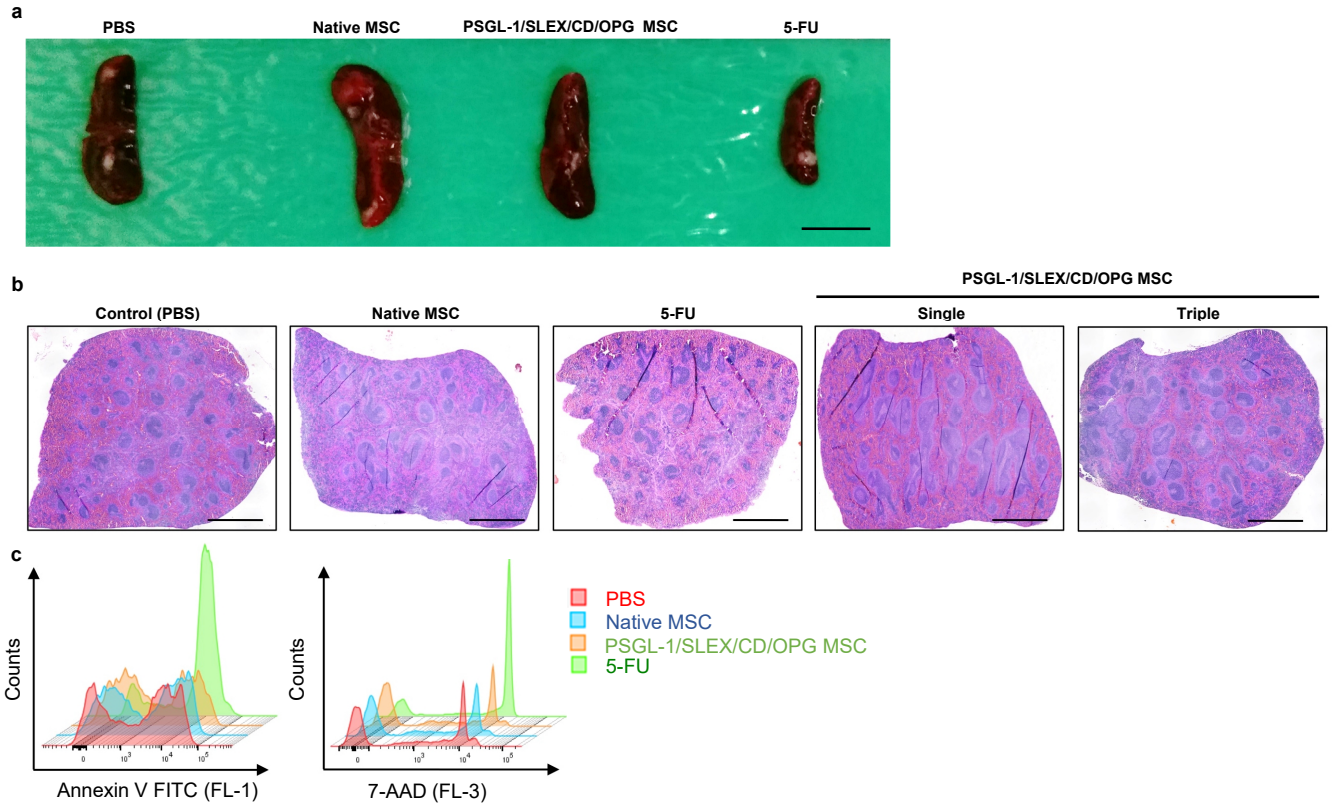

Supplementary Figure 13: MDA-MB231 intratibial model mice infused with PSGL-1/SLEX/CD/OPG MSC via *i.v.* injection exhibited minimal toxicity. (a) 5-Fluorouracil treatment caused spleen reduction. Whole spleens were taken in pictures right after mice euthanasia. Scale bar: 1 mm. (b) 5-Fluorouracil induced toxicity led to death of germinal centres and tissue fibrosis in the mouse spleen. Images show H&E staining on spleen longitudinal sections. Scale bar: 1,000 µm. (c) 5-Fluorouracil treatment induced cell apoptosis and necrosis within the bone marrow. For each group [Control (PBS), Native, PSGL-1/SLEX/CD/OPG MSC + 5-FC and 5-FU], 10,000 cells were analysed. Histograms show Annexin V FITC binding to the cell membrane (FL-1) and 7-AAD staining (FL-3). For Annexin V FITC, the medians of fluorescence of each group were 2,797, 2,204, 1,028, and 9,677, respectively. Whereas for 7-AAD, the medians of fluorescence of each group were: 713, 836, 361, and 10,640, respectively.

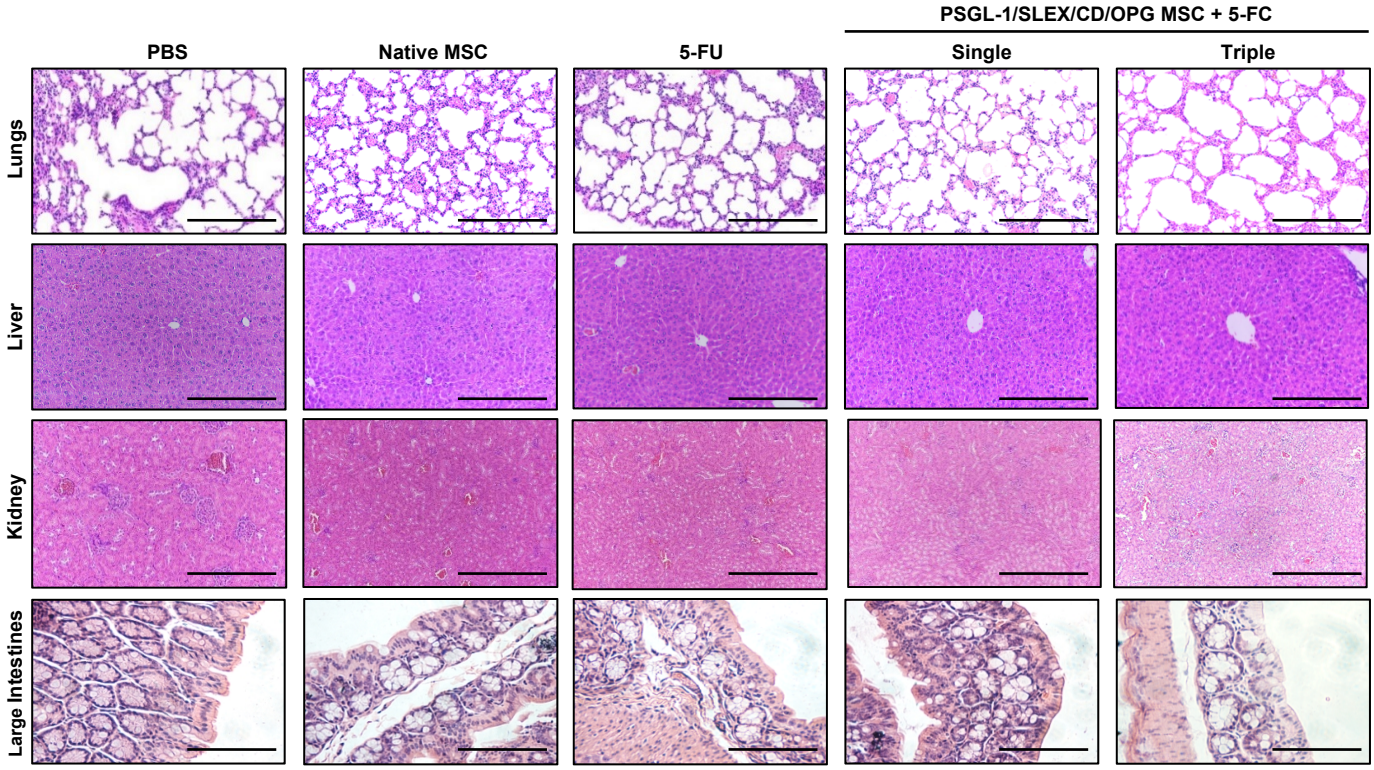

Supplementary Figure 14: MDA-MB231 intratibial model mice infused with PSGL-1/SLEX/CD/OPG MSC via *i.v.* injection exhibited minimal toxicity. Tissue analysis was performed following H&E staining to evaluate toxicity-induced damages. Scale bar: 500 μm for lungs, liver, and kidney, and 250 μm for large intestines.

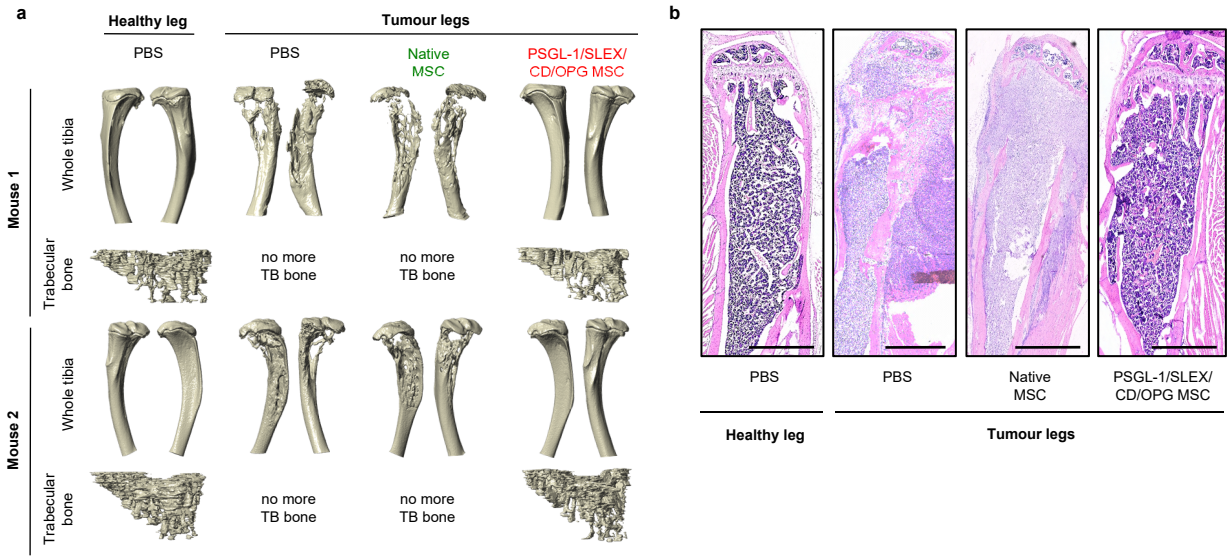

Supplementary Figure 15: Illustrative bone integrity analyses following systemic *i.v.* infusion of PSGL-1/SLEX/CD/OPG MSC in MDA-MB231 intratibial model mice. (a) Representative bone analysis using nanoCT imaging. At the end-point of treatment, mouse tibias were harvested, fixed for 48 h, and tibias of 2 mice per group [Control (PBS), Native MSC and PSGL-1/SLEX/CD/OPG MSC] were analysed. Top panel shows 3D reconstructions of whole tibias (without the fibula) and bottom panel shows 3D reconstruction of trabecular bone. (b) H&E staining was performed on representative tibia sections for each group to assess tumour invasion within the bone marrow and bone integrity. A healthy tibia section is also shown as a reference. Scale bar: 1,000 µm.

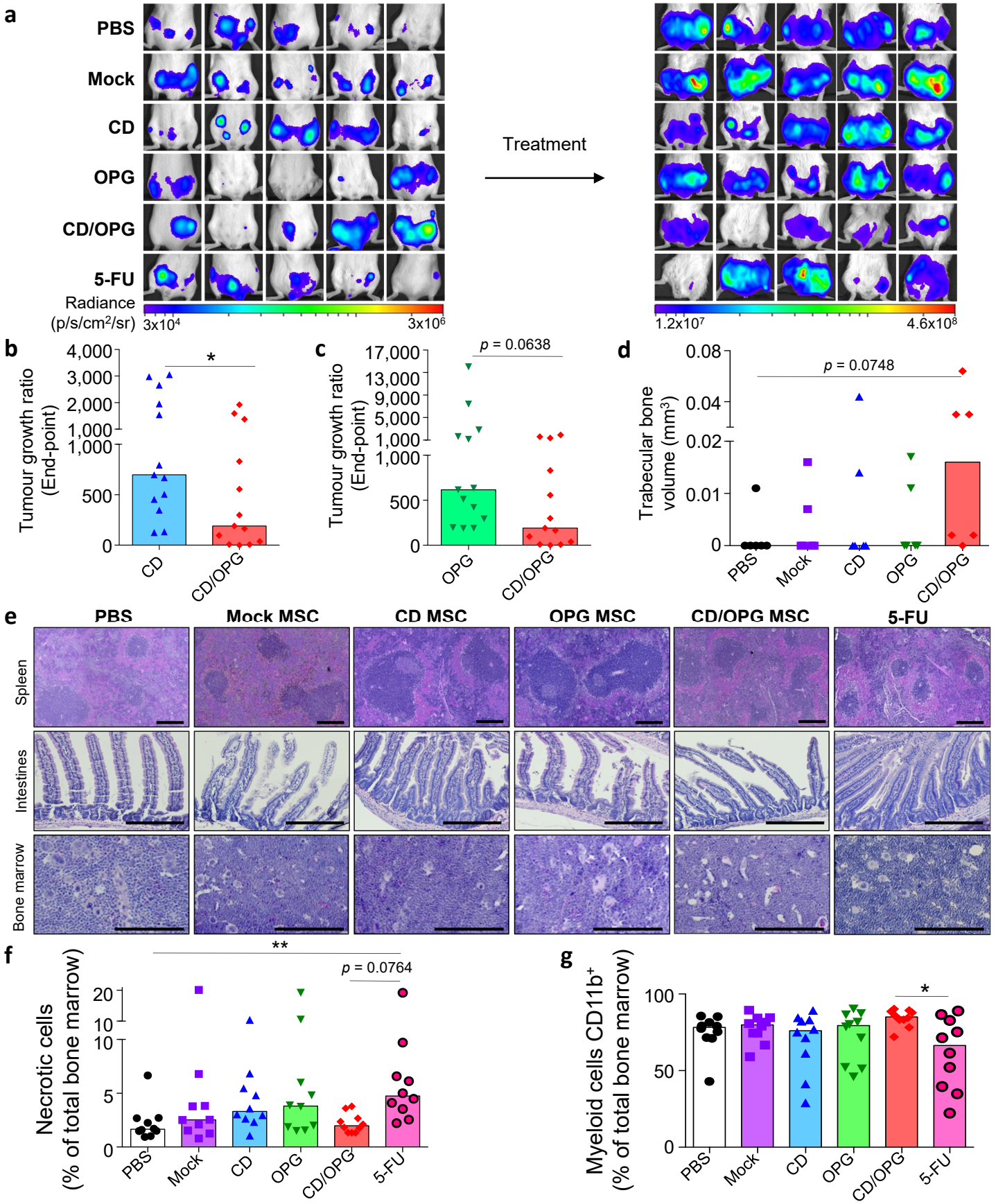

Supplementary Figure 16: PSGL-1/SLEX/CD/OPG MSC exhibit therapeutic effects and minimal toxicity in a syngeneic mouse model of spontaneous bone metastasis. (a) Bioluminescence imaging was done to monitor bone metastasis development. Panel shows tumour signal before and after treatment for 5 representative mice per group. MSC were engineered as follows: Mock group (Mock transfected), CD group (PSGL-1/SLEX/CD), OPG group (PSGL-1/SLEX/OPG), and CD/OPG group (PSGL-1/SLEX/CD/OPG). (b) CD/OPG MSC treatment is more effective than CD MSC in inhibiting tumour growth. All MSC infusions were via *i.v.* injection. Bar graph shows the median tumour growth ratio at the end-point for each group; each point represents one animal. n=13. Statistical analysis: Mann–Whitney, * $p \leq 0.05$. (c) CD/OPG MSC treatment tends to be more effective than OPG MSC in inhibiting tumour growth. Bar graph shows the median tumour growth ratio at the end-point for each group; each point represents one animal. n=13. Statistical analysis: Mann–Whitney, * $p=0.0638$. (d) CD/OPG MSC treatment tends to prevent bone loss in metastatic femurs. Micro-CT was done on n=6 tumour-bearing femurs per group, and remaining trabecular bone volume was quantified. Bar graph shows the median trabecular bone volume for each group; each point represents one animal. Statistical analysis: Kruskal-Wallis with Dunn's multiple comparison *post hoc*, $p=0.0748$ between PBS and CD/OPG MSC. (e) No obvious signs of toxicity were detected in peripheral organs. Spleen, intestines, and bone marrow were analysed for each group using H&E staining. Representative images are shown here. Scale bar = 250 µm. (f) 5-FU treatment, but not MSC groups, induces more necrosis in the bone marrow. At the end-point, the bone marrow of the healthier leg was isolated and cell necrosis was analysed using flow cytometry (7-AAD$^+$) for n=10 animals per group. Bar graph shows the median percent of necrosis for each group, and each point represents one animal. Statistical analysis: Kruskal-Wallis with Dunn's multiple comparison *post hoc*, ** $p \leq 0.01$ between 5-FU and PBS, and $p=0.0764$ between CD/OPG and 5-FU. (g) Engineered MSC are less toxic than 5-FU and induces less reduction of myeloid cells (CD11b$^+$) in the bone marrow. At the end-point, the bone marrow of the healthier leg was isolated, and phenotyping was done on living cells (7-AAD$^-$) using flow cytometry for n=10 animals per group. Bar graph shows the median percent of CD11b$^+$ cells for each group, and each point represents one animal. Statistical analysis: Kruskal-Wallis with Dunn's multiple comparison *post hoc*, * $p \leq 0.05$ between CD/OPG and 5-FU.